FOREX Publication
Open Access | Rapid and quality publishing

International Journal of
Electrical and Electronics Research (IJEER)
Research Article | Volume 11, Issue 4 | Pages 1128-1135 | e-ISSN: 2347-470X

MRI Intracranial Neoplasm Localization Using Convolution Neural Network Based Residual Block ResUnet: A Systematic Approach

Dr. G N Keshava Murthy[1], Dr. Sujata Joshi[2], Dr. Rekha H[3], Dr. Usha B. S[4], Nandini Prasad K. S[5]

[1]Assistant Professor, Department of EIE, Siddaganga Institute of Technology, Tumkur, India.
[2]Associate Professor, Department of CSE, Nitte Meenakshi Institute of Technology, Bangalore, India.
[3]Professor, Department of ISE, Shridevi Institute of Engineering and Technology, Tumkur, India.
[4]Professor, Department of CSE, East West Institute of Technology, Bangalore, India.
[5]Professor, Department of ISE, Dayananda Sagar Academy of Technology and Management, Bangalore, India.

**Correspondence: keshavamurthytg5@gmail.com & gnk@sit.ac.in*

ABSTRACT- Analysis of intracranial neoplasm using multimodal MR images requires accurate and automatic segmentation. However, manually classifying tumors with similar structures or appearances in magnetic resonance imaging (MRI) with similar anatomy or appearances is more challenging, requiring experience to detect brain tumors. Precise segmentation of brain tumors gives clinicians with a foundation for surgical planning and treatment. Due to its capacity to segment brain tumor images automatically, Deep Neural Networks (DNN) have been widely used in image segmentation applications. To classify, segment and marking the occurrence of the brain tumor area accurately, we present custom Deep Convolution Neural Network (CNN) based Residual block U-Net (RB-ResUnet) architecture. Our technique is tested on publicly available Kaggle datasets utilizing quantitative metrics. Comparative results demonstrate that the custom CNN-based RB-ResUnet model can more reliably identify tumor locations and give accurate segmentation masks to tumor locations that are defined by bounding boxes. The findings of the experiment reveal that our proposed model RB-ResUnet can effectively aid in the identification, toxicological evaluation of the brain tumor and has clinical research as well as practical application.

Keywords: Deep learning; Convolution Neural Network; ResU-Net; Residual block; Brain Tumor Segmentation

ARTICLE INFORMATION

Author(s): Dr. G N Keshava Murthy, Dr. Sujata Joshi, Dr. Rekha H, Dr. Usha B. S, Nandini Prasad K. S;
Received: 22/08/23; **Accepted:** 05/11/23; **Published**: 19/12/2023;
E- ISSN: 2347-470X;
Paper Id: IJEER230727;
Citation: 10.37391/IJEER.110433
Webpage-link:
https://ijeer.forexjournal.co.in/archive/volume-11/ijeer-110433.html

crossref member
CROSSREF.ORG
THE CITATION LINKING BACKBONE

Publisher's Note: FOREX Publication stays neutral with regard to jurisdictional claims in Published maps and institutional affiliations.

1. INTRODUCTION

An intracranial neoplasm, more commonly referred to as a brain tumor, occurs by the proliferation of aberrant brain cells. In light of the time and effort required to manually segment brain tumors from MRI images, automatic segmentation is preferable over manual segmentation. The area of automatic segmentation of brain tumors is undergoing extensive development. Brain tumors are extremely dangerous to one's health and can result in death. The patient's age, tumor type, and location all factor into the treatment plan for their brain tumor. Tumors can grow and spread to healthy tissue nearby, making it difficult to diagnose and treat. Thus, Automatic segmentation leads to early prediction of tumor in the brain suggests a faster response in therapy, which helps to enhance patients' survival rates. Over the last few decades, medical researchers have found over 120 different forms of brain tumors. There are two forms of brain cancers: primary brain tumors that originate in the brain, and secondary brain tumors that arise when the underlying tumor is elsewhere in the body [1]. Various imaging methods such as MRI, PET, and CT scans are used to identify these tumors. One of these is MR Imaging technique, which, when compared to other imaging modalities, has shown promising results in the proper detection and diagnosis of health problems in patients. Furthermore, Temporary exposure to MR environment poses no recognized health risks. Thus, MRI is a useful tool for human brain tumor access. Magnetic resonance imaging (MRI) image anomaly detection by hand is a time-consuming and difficult task [2]. Tumors require rapid medical attention, which is difficult to detect using manual seg- mentation. Brain tumor segmentation is best diagnosed by using artificial segmentation algorithms with higher dice score coefficient [3].

The edges of the tumor are typically hazy, and the tumors may expand into adjacent parts of the brain, making it difficult to distinguish the afflicted tissue from the healthy tissue surrounding it. Delineating tumor boundaries manually in MRI data is immoderate task and prostrate to inaccuracy. Segmentation of brain tumors automatically incorporating MRI scans would overcome these obstacles by determining the type and precise location of tumors. Early tumor treatment can cure patients. Deep learning (DL) algorithms have played a critical role in the efficient segmentation of brain tumors in recent research focused on the establishment of efficient and accurate

FOREX Publication
Open Access | Rapid and quality publishing
International Journal of
Electrical and Electronics Research (IJEER)
Research Article | Volume 11, Issue 4 | Pages 1128-1135 | e-ISSN: 2347-470X

automated segmentation approaches. Convolution Neural Networks (CNNs) are the most prevalent and well-known DL models because of their weight-sharing nature, which allows them to learn dense properties from training data [4]. DL-based brain tumor segmentation has caught the interest of researchers because of these benefits [5]. Patch-based CNN [6], multi-scale diagnostics CNN [7], DCNN [8], a fully convolution-based CNN (FCNN) [9] based on patches, and models for tumor segmentation based on the U-net are all relevant works. Image content and label correlation are reduced by using only a small section of the scan as a CNN information and categorizing a unique class to each patch [10]. However, probability distributions can be predicted using an enhanced variation of the CNN known as FCNN by pixel rather than by patch [11]. This improvement allows FCNN to anticipate the full image in a single forward pass by taking a full-sized image. Existing DL-based approaches, despite recent developments, are grown computationally expensive due to the use of numerous convolution layers and kernels. Consequently, the need for a more effective approach for identifying and segmenting tumors using less memory and processing resources is still present [12].

The purpose of this research is the development of a framework for instance segmentation that is comparable in terms of ease of use. Since accurate recognition of all objects in a picture and precise segmentation of each instance are required for instance segmentation, it is an arduous assignment to accomplish successfully. The Semantic-segmentation and object detection are thus combined in this work, with the purpose of classifying and localizing individual items using a bounding box in the classical computer vision tasks. Object detection is used to classify and localize objects using bounding boxes as shown in *figure.1*.

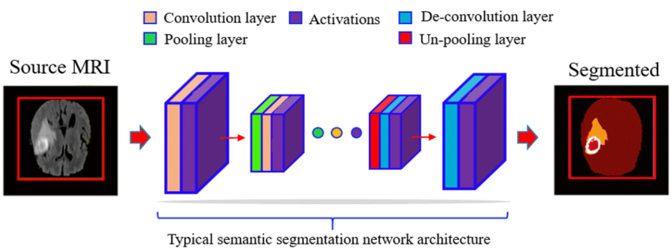

Figure 1. The simple CNN for semantic segmentation

Using MRI scans, we provide in this study a method for automatically detecting and segmenting brain tumors. Comprehensive training of a ConvNets is accomplished using the multitask loss function and the residual U-Net model [13] with dense residual blocks and skip connections, both of which are derived from the residual block and skip connection features of the model.

The Dense-ResUNet consists of dense convolutional blocks nested within each other and a Residual connection in the U-Net model. Prior to fusion, it is possible to connect the encoder and decoder feature maps using nested dense convolutional blocks (NDCBs), allowing many levels of features to be completely utilized. The deep traditional CNN network problem can be addressed using residue blocks and skim connections, images that can be used to get information about the pixels and skip the link. In order to demonstrate the model's efficacy, we used multiple quantitative measures using publicly available kaggle brain tumor datasets [14]. In recent re- search, a Residual U-Net model was used to detect as well as segment 3D brain pictures [15], oral illness [16], breast and lung tumors [17, 18]. The following are the most significant contributions made by the planned work:

1. MRI brain tumors can be accurately segmented and classified even in the existence of noise, distortion, and bias field-effect fluctuations in the raw images, by applying pre-processing steps to the proposed method.
2. Due to the lack of a boundary box and the obfuscation of ground truths (GTs) in publicly available information, we created annotations that are required for training the proposed model.
3. The precise detection and segmentation of tumour regions using a DenseNet-based ResU-Net that operates end-to-end.
4. In order to demonstrate the framework's resilience, we ran extensive tests on kaggle MRI brain tumour datasets, comparing the findings to those produced by other existing techniques.

2. LITERATURE SURVEY

The development of an automated model is an important innovative field because of the high clinical value and complexity of the brain tumor. This section provides a brief overview of current efforts to identify and categorize malignancies of the brain using MR images. The comparison of DL-based methods to the segmentation of medical imagery has showed promise in recent years [19]. A more robust feature vector can be generated by autonomously learning complex feature representations from training data. Down-sampling and a fully linked CRF network were utilized as post-processing in the Kamnitsas et al. [20] 3D CNN design, which considers 3D patches and global contextual information. The authors [21] proposes an extended DeepMedic with residual connection for tumor segmentation. To categorize the individual patches in MRI images, CNN-based approaches for brain tumor segmentation use small regions from the images to segment them [22]. Using FCNNs to segment both natural and medical images has showed promising results over the last few years [23]. FCNN uses convolutional kernels rather than layers that are not fully connected. The image's original size can be recovered by the use of up-sampling and de-convolution layers. Furthermore, end-to-end training is performed on the model and is highly efficient than patch-level classification approaches. In image segmentation, the encoder-decoder framework is a common one. The image's pixels are generalized to a 3D distribution during the encoding task, and the image's details and spatial dimensions are gradually restored during the decoding process. As a result, the encoder-decoder structure enables complete semantic segmentation of the image [24]. To minimize image size and broaden the receptive area of the Convolutional neural networks, they use pooling and followed by up-sampling to the initial in semantic image segmentation. As part of the procedure, certain image details are lost [25]. A

U-net architecture, developed by Oktay et al. [26], has attention gates that automatically adjust focus to different-sized target structures. During training, the target region's attention density increased, while background region's attention density decreased, improving segmentation accuracy. Don et al. [27] segmented tumors using a U-net CNN architecture minor modifications. They improved segmentation accuracy by combining artificial data augmenting with a loss function based on dice. Using encoder–decoder architecture revealed the sectioning out of the tumor from the brain's regular neurons on a pixel-by-pixel basis was demonstrated in [28]. SegNet architecture with a depth four encoder and a VGG16 feature map generator was utilized to generate feature maps, and non-linear up-sampling was conducted. Dice scores of 0.931 on average were obtained using this method, which does not require any post-processing.

The researcher in [29] proposed a SegNet for automatic brain tumor segmentation after post-processing. First, the inputs are normalized and bias field corrected to reduce undesirable artifacts, improving segmentation performance. Each of the four MRI modes is trained separately using SegNet. The encoder (downsampling) and decoder (upsampling) (upsampling). The encoder employs 13 convolutional layers with three-dimensional (3x3) filters, BN, ReLU, and max-pooling layers with two-dimensional (2x2) filters. The decoder has 13 Convolutional layers, which correspond to the layer count upon the encoder. Decoder high dimensionality features are given to softmax layers for class pixel classification. The approach attained 85% accuracy for the total tumour, 80% for the core tumour, and 79% for the augmenting tumor [30]. The Mask Region-based CNN (Mask R-CNN) approach [31] to bounding-box object detection focuses on a manageable number of potential object regions [32] and assesses convolutional networks [33] separately on each RoI. To forecast a segmentation mask, each RoI has a tiny FCN applied. It is easy to set up and train Mask R-CNN using the Faster R-CNN framework. As a result, a fast system and rapid experimentation are possible. Residual blocks [34], added by researcher to the UNet, aid in the extraction of additional characteristics at each layer. Res-UNet is frequently used as a foundation model for numerous Deep Learning architectures because of its superior performance and efficacy in feature extraction [35]. Recent segmentation techniques have been developed to address the CNN redundancy problem by assigning a class label to each pixel and modify the architecture to Fully Convolutional Network (FCN). Each of the image's local blocks is classified by a U-shaped design with expanding and contracting routes.

This method requires a huge number of training brain scans in order to successfully segment the brain, however GPU memory limits the number of images that can be used, and pixel-wise computations result in long processing times. The authors in adopted a similar architecture to Unet's, but modified the layers of contraction and extending routes accordingly. In the original U-shaped FCN, they recommended residual blocks instead of convolute blocks. Each of the blocks comprises two convolutional units, a layer of BN and PReLU activation function. These strategies improve segmentation outcomes but require excessive pixel-wise computing time. The Figure 2 shows U-Net architectural representation for process of image segmentation.

To overcome limitations recognized in CNN, FCN, and ResNets, this research employs CNN based RB-ResNets The idea behind RB-ResU-Nets is to add the layer's output to its input. This minor modification helps deep network training since they have parallel shortcut connections to convolutional layers. This study presents a segmentation network with multi-modal nested dense ResU-Nets and tests its efficiency on freely available database of brain tumors. The objective of this article is, with the use of their mask images, learn to distinguish between MRI brain images with and those without tumors by using a classifier, and segment the tumor from normal brain tissues.

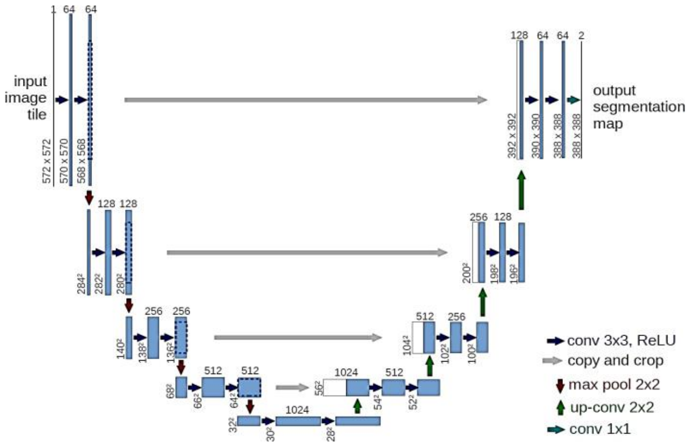

Figure 2. The Image Segmentation U-Net Architecture

3. METHODS AND MATERIALS

This section depicts the detailed outline of our proposed method CNN-based ResU-Net architecture in detecting brain tumors. In addition, this part explains the dataset, preprocessing methods, and further implementation details of the Dense CNN-based ResU-Net with dense residual blocks. *Figure 3* illustrates the proposed methodology's workflow. The presented DL approach uses CNN-based RB-ResUnet to accurately locate, segment, and classify brain tumors. Our goal is to detect a brain tumor in an MRI image without manual intervention.

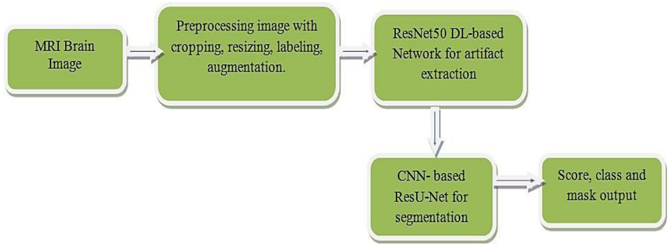

Figure 3. The Flow Diagram Proposed Methodology

MRI-induced noise and artifacts are removed from the input images before they are used in the further analysis. Then the model is trained using ground truth segmentation masks. Following that, a proprietary ResU-Net model is employed to determine the location, classification, and segmentation of

International Journal of
Electrical and Electronics Research (IJEER)
Research Article | Volume 11, Issue 4 | Pages 1128-1135 | e-ISSN: 2347-470X

tumors. The ResNet50 CNN based pre-trained model is adopted in the exploitation of raw artifacts from the input brain image. The image's complex structure can't be captured by a shallow convolution structure, yet the stack's deep convolution and redundant structure cause gradients to disappear and tear. Instead of making a connection, we utilize a residual unit to extract pixel data from the image to circumvent standard DCNN network difficulty. Figure 4 depicts the structure of the residual unit.

3.1 MRI Brain Dataset

The suggested approach is evaluated and verified on the Kaggle Multimodal Brain Tumor Segmentation dataset. There are 352 images of tumours in the brain and 139 images of healthy people in the dataset. To ensure accuracy, the expert labels the ground truth on each of the large MRI scans. There are four labels for distinct forms of brain tumors in our suggested model: no tumour (labelled 3), pituitary tumor (labelled 2), meningioma tumor (labelled 1), and glioma tumor (labeled 0). Glioma, meningioma, and a pituitary brain tumor can all be shown in MRI images in *figure 4*.

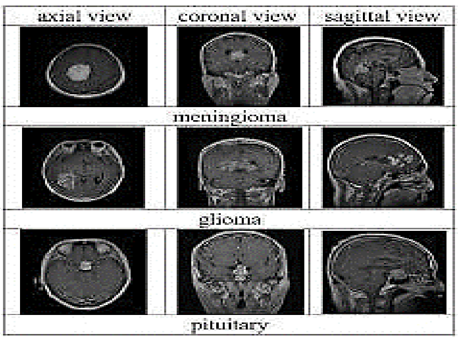

Figure 4. MRI Brain Tumor types

3.2 Data Preprocessing

One of the most well-known effects on MR Imaging scans is inclination field contortion. Each individual patient underwent four MRI scans. We used the N4ITK technique, to rectify bias field distortion. Patient-to-patient variability exists with regard to the intensity distribution. As a result, we apply intensity Z-score intensity normalization method on an individually sequenced basis to normalize pixel level intensities among patients. After that, the extracted patches are normalized with each MRI brain images in order to have mean of zero with an equal variance and can be computed as in *equation (1).*

$$Z' = \frac{Z-\mu}{\delta} \tag{1}$$

where 'z' is the input image, 'z' - normalized scan, 'μ' reflects the image's median value and 'δ'- standard deviation of the image data.

3.3 Train, Test and Validation dataset allocation

Three subsets of the MRI brain dataset have been created for the purpose of training, validating, and testing. In order to test the suggested model, the training data is used. Hyper-parameters of the model that is produced from the training set are fine-tuned using the validation set. Indirectly, the validation process has an effect on the resulting model. The test set is a part of database that is used to objectively evaluate the model that was constructed. Accordingly, 10% of the dataset was randomly assigned to the test set. The validation set receives 10% of the remaining dataset and the model is trained with remaining 80% of data. The implementation of database split up as in *figure 5*.

```
[ ]  # split the data
     from sklearn.model_selection import train_test_split
     def split_data(data):
         train_data, test_data = train_test_split(data, test_size=0.15)
         train_data, val_data = train_test_split(train_data, test_size=0.15)
         return [train_data, val_data, test_data]

     glioma_data = split_data(glioma_tumor)
     meningioma_data = split_data(meningioma_tumor)
     pituitary_data = split_data(pituitary_tumor)
     normal_data = split_data(normal)
```

Figure 5. MRI Brain Tumor Dataset Split into Train, Validate and Test Set

3.4 Annotations

The Ground Truth (GT) mask on each MRI picture helps the trainer identify the tumor part. The MRI images are annotated using the VGG Image Annotator (VIA). *Figure 6* is a comparison of the raw image and its GT counterpart. When the interpretations of VIA are saved in a JavaScript Object Notation file, a region value of 0 or 1 is assigned to each of the tumor polygon points. For a tumor region, pixels inside the enclosing polygon get a value of 1, while outside pixels are assigned 0 value. For each MRI image used in training, this file is utilized to create a mask image.

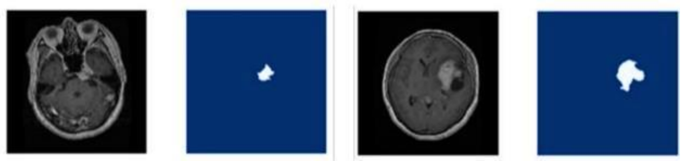

Figure 6. Raw MRI Brain Image with GT Mask

3.5 ResNet-50 CNN Classification Model

One of the DCNN models is ResNet50, also known as Residual Network with 50 convolution layers. To make our proposed model more accurate, the Resnet50 model is utilized as a base. Microsoft launched the residual network in 2015. The Resnet50 model has demonstrated success in biomedical data with effective brain tumor classification results. But a degradation problem emerges as the layers count in a deep nets increase. Moreover, layer's weights cannot be updated effectively to the subsequent layer. In addition to the standard convolutional layers, ResNet50 employs short connections to circumvent this issue. The residual building block unit seen in *figure 7* has a short connection. The H(X) is the residual block's output expression is represented in *equation (2)*.

$$F(X) = H(X) - x \tag{2}$$

Equation (3), for the stocked nonlinear weight layer F(x) is shown below:

$$H(X) = F(X) + x \tag{3}$$

FOREX Publication
Open Access | Rapid and quality publishing
International Journal of Electrical and Electronics Research (IJEER)
Research Article | Volume 11, Issue 4 | Pages 1128-1135 | e-ISSN: 2347-470X

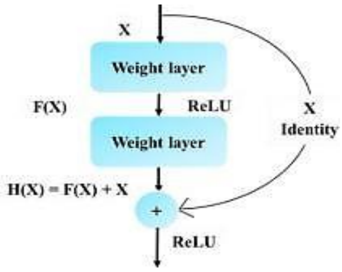

Figure 7. The Residual unit framework

Input, Padding, Convolution, Batch Normalization, Activation (ReLu), and Max Pooling are the layers that make up the residual network in our research study. Besides these, the model has been enhanced with extra tiers. Averaging, Flattening, Dense Dropout and Flattening are the four additional layers that are being added to enhance the hyper-parameters count that may be trained. Each individual convolution layers includes feature maps. The ReLu activation function expresses semantic image properties with content and space when the convolution kernel scans a pixel in the image for feature extraction as in *equation (4).*

$$Y_j^{m+1} = f(t_i^{m+1} + \sum_{i \varepsilon j} X_i^m * k_{ij}^{m+1}) \qquad (4)$$

Where, input feature 'Xi' in layer (l+1) is represented by 'Y_j', 'f'- ReLU (rectifier linear unit) activation function, 'e_j' represents input eigen-matrices, '*' - convolution operation, and 'k' - convolution kernel. Image characteristics can be reduced in dimension using the Max pooling layer to transmit high-level content and semantics operation in *equation (5).*

$$Y_j^{m+1} = f(t_j^{m+1} + X_j^m \otimes k_j^{m+1}) \qquad (5)$$

Where, max pooling layer operation is indicated by '⊗' in the CNN structure. Lastly, as the prediction layer, the fully connected layer employs the maximum likelihood function to perform MRI brain image classification. *Figure 8.* illustrates ResNet50 architecture in classifying the tumor.

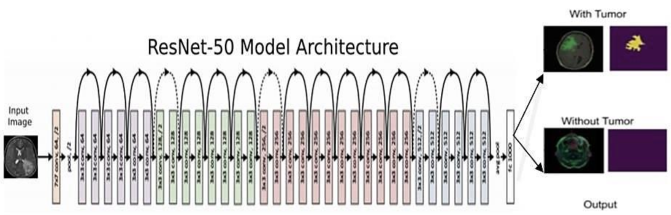

Figure 8. The ResNet-50 architecture.

3.6 CNN – Based MRI ResU-Net Segmentation Method

The segmentation model CNN-based RB-ResUnet is a hybrid model that combines the benefits of both U-Net and ResNet models in a single model. The residual unit reduces the hyper-parameters needed to train the CNN by skipping connections between low and high levels of the network. The ResU-net is made up of three separate pathways.

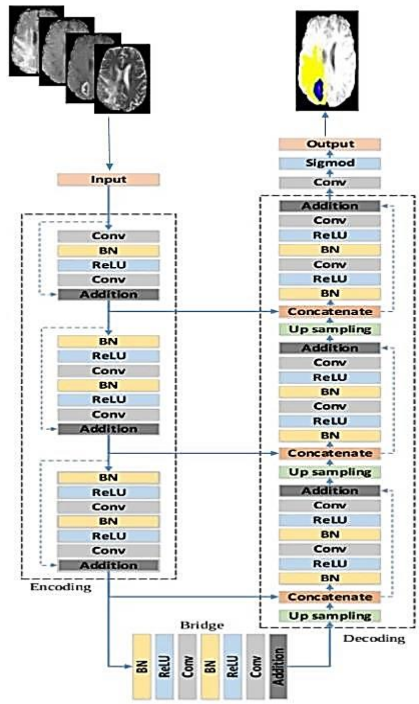

Figure 9. CNN-based RB-ResUNet architecture.

There are three ways to represent data: encoding, which compresses the input, and decoding, which does the reverse and organizes the representation by pixels. Then there's the Bridge, which connects the two channels. The decoding which is opposite of encoding and categorizes the representation in a pixel-wise form and the bridge which joins the two paths together are the three main components of the system. Each residual unit consists of dual 3x3 convolution blocks, ReLu, Batch normalization, convolution and pooling layers and identity mapping.

Figure 9 shows the CNN-based RB-ResUnet architectural representation for segmenting the region of brain tumor.

4. EXPERIMENTAL RESULT

This part delves deeply into the analysis and discussion of the data gathered. We conducted experiments publicly available kaggle datasets of MRI brain scans. The proposed methodology employs two distinct deep NNs, ResNet50 and ResU-net, as cornerstone networks for autonomously learning deep the intricacies shown by training images and localization of tumor area in MRI brain scan.

4.1 Results and Analysis

In order to segment the brain tumor, we employ a CNN-based RB-ResUNet. When used with brain masks, it can identify the ROI on MRI scans, which allows it to isolate the brain tumor from its surrounding areas. At first, we used ResNet-50 model to identify and classify the tumor type as, glioma, meningioma, pituitary brain tumor or no tumor with predicted mask. When there is no tumor, then the Boolean variable has_mask = 0 or 1 if there exists the tumor. *Figure 10* represents the outcome of prediction model.

FOREX Publication
Open Access | Rapid and quality publishing
International Journal of
Electrical and Electronics Research (IJEER)
Research Article | Volume 11, Issue 4 | Pages 1128-1135 | e-ISSN: 2347-470X

Secondly, based on the outcome of the ResNet-50, if there exists the tumor in the brain, then we used our proposed model CNN based RB-ResUnet to segment and localize the tumor's ROI of affected area in the MRI scan of brainstem cerebrum. The segmented model is trained on MRI scans after extracting ROI along with tumor's masks from the ResNet-50.

The *section 4.2* illustrates the data visualization of RB-ResUnet segmentation model. To assess the CNN based RB-ResUnet model's performance, accuracy and error rate are examined in this section.

	image_path	predicted_mask	has_mask	Tumor Type
0	n (156).jpg	No mask :)	0	No tumor detected
1	n (6).jpeg	No mask :)	0	No tumor detected
2	n (13).jpg	No mask :)	0	No tumor detected
3	n (12).jpg	No mask :)	0	No tumor detected
4	/content/drive/MyDrive/BT/TRAIN/y (1).png	[[[[5.5184508e-08], [1.4039009e-07], [1.309600...	1	Tumor Detected :Most likely Meningioma Tumor
5	/content/drive/MyDrive/BT/TRAIN/y (48).jpg	[[[[8.14559e-08], [2.9701596e-07], [3.2375948e...	1	Tumor Detected :Most likely Glioma Tumor
6	y (38).jpg	No mask :)	0	No tumor detected
7	/content/drive/MyDrive/BT/TRAIN/y (47).jpg	No mask :)	0	Tumor Detected :Most likely Glioma Tumor
8	/content/drive/MyDrive/BT/TRAIN/y (39).jpg	[[[[1.1383825e-07], [3.491739e-07], [3.6133036...	1	Tumor Detected :Most likely Glioma Tumor
9	/content/drive/MyDrive/BT/TRAIN/y (26).jpg	[[[[1.1452285e-07], [3.5113342e-07], [3.645260...	1	Tumor Detected :Most likely Glioma Tumor
10	/content/drive/MyDrive/BT/TRAIN/y (14).jpg	[[[[1.0291296e-07], [3.3976752e-07], [3.322293...	1	Tumor Detected :Most likely Glioma Tumor
11	/content/drive/MyDrive/BT/TRAIN/y (10).jpg	No mask :)	0	Tumor Detected :Most likely Glioma Tumor
12	/content/drive/MyDrive/BT/TRAIN/y (15).jpg	[[[[1.1103778e-07], [3.4323634e-07], [3.537001...	1	Tumor Detected :Most likely Glioma Tumor

Figure 10. ResNet-50 Predicting the Category of Tumor Type

An Accuracy of 96.8 percent was achieved by evaluating our Kaggle MRI brain dataset against the model with the increase in number of epochs and less error rate.

4.2 Output Data Visualization

Figure 11 illustrates a portion of the processed dataset. It displays the raw MRI brain tumor picture, with the Artificial Intelligence (AI) predicted mask after implementing and trained our proposed system on dataset after ResNet-50 classification model.

The R B-ResUNet improves the accuracy of outcomes by making use of the model as in *figure 12*.

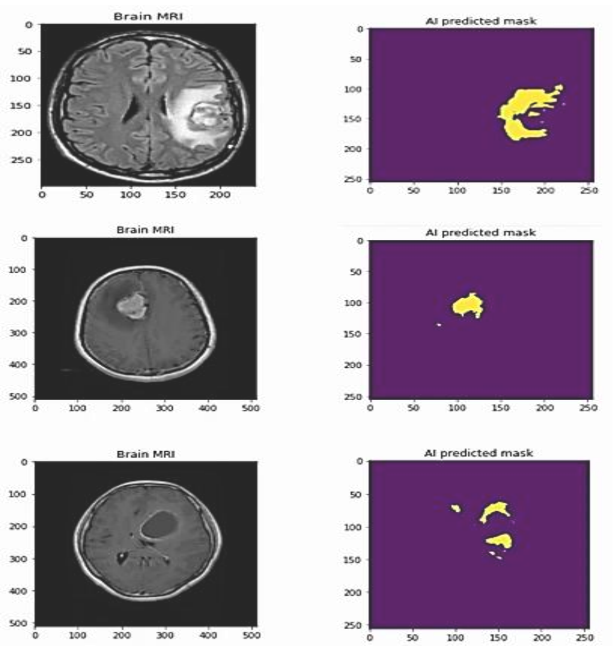

Figure 11. The ROI localization of tumor from MRI scan by RB-ResUNet Model.

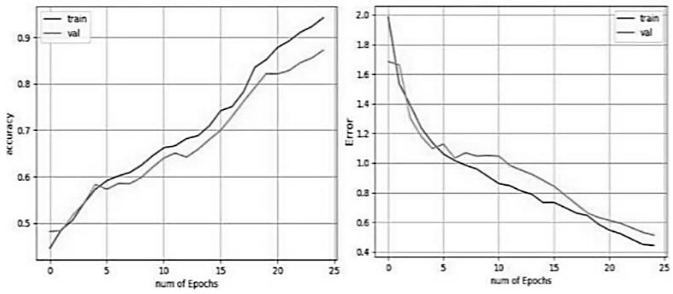

Figure 12. Training vs validation metrics with epochs = 25

4.2 Performance comparison with other existing methodology

Table 1 compares the proposed method's overall accuracy to some selected work from the literature, based on the results stated in their published papers, in order to provide additional insight on the results. In comparison to earlier research, our strategy yielded significantly higher accuracy on Kaggle Brain MRI dataset.

Table 1. Comparative Analysis with Existing Technologies

Application	Methodology adopted	Accuracy obtained
Author [31]	Deeper Residual block Learning Network	90%
Author [12]	BU-Net architecture	91%
Author [22]	ReSoU-network	87.6%
CNN based RB-ResU-net (ours)	Deep Residual U-Network	96.8%

5. CONCLUSION

The major objective of this investigation is to develop an efficient autonomous brain tumor segmentation and localization system with a high degree of accuracy, performance, and simplicity. To begin, the usual classification of brain tumors is accomplished using a CNN along with ResNet50 architecture. The classification results in a determination of whether a tumor exists or not. When the tumor exists, our model also classifies the tumor type as glioma, meningioma or pituitary tumor. Although the complexity is low, the calculation time is lengthy, the accuracy is likewise lengthy. Additionally, to localize the tumor in the given image and to draw an edge around it, another segmentation technique, namely CNN based RB-ResUNet segmentation, is used to carry out the suggested scheme's localization of the tumor. The results display brain MRI scans with the tumor's projected location in the form of a mask. The accuracy of the training is 97.8 percent. Due to the critical nature of the physician's diagnosis, the overall accuracy of the physicians will aid in diagnosing the tumor and treating the patient with enhanced precision using the proposed method.

DATA AVAILABILITY STATEMENT

The research findings are investigated with online publicly accessible available online Kaggle datasets at https://www.kaggle.com/preetviradiya/brian-tumor-dataset .

ACKNOWLEDGMENTS

Dayananda Sagar Academy of Technology and Management and East West Institute of Technology, Bengaluru, India, supported to complete research work.

REFERENCES

[1] N. A. Prasad and C. D. Guruprakash, "An ephemeral investigation on energy proficiency mechanisms in WSN," 2017 3rd International Conference on Applied and Theoretical Computing and Communication Technology (iCATccT), Tumkur, 2017, pp. 180-185.

[2] R. V S and Siddaraju, "Defective Motes Uncovering and Retrieval for Optimized Network," 2022 6th International Conference on Computing Methodologies and Communication (ICCMC), 2022, pp. 303-313, doi: 10.1109/ICCMC53470.2022.9754109.

[3] P. N and C. D. Guruprakash, "A Relay Node Scheme for Energy Redeemable and Network Lifespan Enhancement," 2018 4th International Conference on Applied and Theoretical Computing and Communication Technology (iCATccT), Mangalore, India, 2018, pp. 266-274.

[4] Manjunatha Kumar, B. H., Achyutha, P. N., Kalashetty, J. N., Rekha, V. S., & Nirmala, G. (2022). Business analysis and modelling of flight delays using artificial intelligence. International Journal of Health Sciences, 6(S1), 7897–7908. https://doi.org/10.53730/ijhs.v6nS1.6735.

[5] M. Digennaro, D. Sambiasi, S. Tommasi, B. Pilato, S. Diotaiuti, A. Kardhashi, G. Trojano, A. Tufaro,

[6] A.V. Paradiso, Hereditary and non-hereditary branches of family eligible for BRCA test: cancers in other sites, Hereditary cancer in clinical practice 15 (1) (2017) 1–5.

[7] Achyutha Prasad, N., Guruprakash, C.D., 2019. A relay node scheme of energy redeemable and network lifespan enhancement for wireless sensor networks and its analysis with standard channel models. International Journal of Innovative Technology and Exploring Engineering 8, 605–612.

[8] Hu, K.; Gan, Q.; Zhang, Y.; Deng, S.; Xiao, F.; Huang, W.; Cao, C.; Gao, X. Brain Tumor Segmenta- tion Using Multi-Cascaded Convolutional Neural Networks and Conditional Random Field. IEEE Access 2019, 7, 92615–92629.

[9] Rekha VS, Siddaraju., "An Ephemeral Analysis on Network Lifetime Improvement Techniques for Wireless Sensor Networks", International Journal of Innovative Technology and Exploring Engineering, vol. 8, issue 9, 2278-3075, pp. 810–814, 2019.

[10] P. K. Pareek, A. P. N, C. Srinivas and J. B. N, "Prediction of Rainfall in Karnataka Region using optimised MVC-LSTM Model," 2023 IEEE International Conference on Integrated Circuits and Communication Systems (ICICACS), Raichur, India, 2023, pp. 1-8, doi: 10.1109/ICICACS57338.2023.10100324.

[11] Achyutha Prasad, N., Guruprakash, C.D., 2019. A relay mote wheeze for energy saving and network longevity enhancement in WSN. International Journal of Recent Technology and Engineering 8, 8220–8227. doi:10.35940/ijrte.C6707.098319.

[12] S. Bhattacharyya, H. Rekha, S. Sarkar, N. Achyutha Prasad, B. N. Jagadeesh and S. Verma, "2.4 GHz Operational PSI-Shaped Patch Antenna Design for Multi-Purpose Applications," 2023 2nd International Conference on Smart Technologies and Systems for Next Generation Computing (ICSTSN), Villupuram, India, 2023, pp. 1-6, doi: 10.1109/ICSTSN57873.2023.10151612.

[13] Rekha, V.S., Siddaraju (2023). Goodness Ratio and Throughput Improvement Using Multi-criteria LEACH Method in Group Sensing Device Network. In: Kumar, A., Senatore, S., Gunjan, V.K. (eds) ICDSMLA 2021. Lecture Notes in Electrical Engineering, vol 947. Springer, Singapore. https://doi.org/10.1007/978-981-19-5936-3_50.

[14] N. G and G. C. D, "Unsupervised Machine Learning Based Group Head Selection and Data Collection Technique," 2022 6th International Conference on Computing Methodologies and Communication (ICCMC), 2022, pp. 1183-1190, doi: 10.1109/ICCMC53470.2022.9753995

[15] Achyutha Prasad, N., Guruprakash, C.D., 2019. A two-hop relay battery aware mote scheme for energy redeemable and network lifespan improvement in WSN. International Journal of Engineering and Advanced Technology 9, 4785–4791. doi:10.35940/ijeat.A2204.109119.

[16] G. T and U. N. L, "Routing and Security in Wireless Ad-Hoc Networks: State of the Art and Recent Advances," 2023 IEEE Renewable Energy and Sustainable E-Mobility Conference (RESEM), Bhopal, India, 2023, pp. 1-8, doi: 10.1109/RESEM57584.2023.10236306.

[17] S. Chaudhury, N. Achyutha Prasad, S. Chakrabarti, C. A. Kumar and M. A. Elashiri, "The Sentiment Analysis of Human Behavior on Products and Organizations using K-Means Clustering and SVM Classifier," 2022 3rd International Conference on Intelligent Engineering and Management (ICIEM), 2022, pp. 610-615, doi: 10.1109/ICIEM54221.2022.9853128.

[18] P. B.D, A. Prasad N, Dhanraj and M. T N, "Adaptive Voting Mechanism with Artificial Butterfly Algorithm based Feature Selection for IDS in MANET," 2023 IEEE International Conference on Integrated Circuits and Communication Systems (ICICACS), Raichur, India, 2023, pp. 1-7, doi: 10.1109/ICICACS57338.2023.10099861.

[19] Nirmala, G., Guruprakash, C.D. (2023). An Overview of Data Aggregation Techniques with Special Sensing Intelligent Device Selection Approaches. In: Kumar, A., Senatore, S., Gunjan, V.K. (eds) ICDSMLA 2021. Lecture Notes in Electrical Engineering, vol 947. Springer, Singapore. https://doi.org/10.1007/978-981-19-5936-3_58.

[20] G. T., R. V., and U. K, N. L., "Detecting Security Threats in Wireless Sensor Networks using Hybrid Network of CNNs and Long Short-Term Memory", Int J Intell Syst Appl Eng, vol. 12, no. 1s, pp. 704–722, Sep. 2023.

[21] Achyutha Prasad N., Chaitra H.V., Manjula G., Mohammad Shabaz, Ana Beatriz Martinez-Valencia, Vikhyath K.B., Shrawani Verma, José Luis Arias-Gonzáles, "Delay optimization and energy balancing algorithm for improving network lifetime in fixed wireless sensor networks", Physical Communication, Volume 58, 2023, 102038, ISSN 1874-4907.

[22] Mohan, B. R.., M, D.., Bhuria, V.., Gadde, S. S.., M, K.., & N, A. P. (2023). Potable Water Identification with Machine Learning: An Exploration of Water Quality Parameters. International Journal on Recent and Innovation Trends in Computing and Communication, 11(3), 178–185. https://doi.org/10.17762/ijritcc.v11i3.6333.

[23] Prasad N. Achyutha, Sushovan Chaudhury, Subhas Chandra Bose, Rajnish Kler, Jyoti Surve, Karthikeyan Kaliyaperumal, "User Classification and Stock Market-Based Recommendation Engine Based on Machine Learning and Twitter Analysis", Mathematical Problems in Engineering, vol. 2022, Article ID 4644855, 9 pages, 2022. https://doi.org/10.1155/2022/4644855.

[24] Ronneberger, O.; Fischer, P.; Brox, T. U-Net: Convolutional Networks for Biomedical Image Seg- mentation. In Proceedings of the International Conference on Medical Image Computing and Computer-assisted Intervention, Munich, Germany, 5–9 October 2015; pp. 234–241.

[25] Murthy, R. K., Dhanraj, S., Manjunath, T. N., Achyutha, P. N., Prasad, A. N., & Gangambika, G. (2022). A survey on human activity recognition using CNN and LSTM. International Journal of Health Sciences, 6(S7), 3408–3417. https://doi.org/10.53730/ijhs.v6nS7.12479.

[26] Prakash, N. C. P., Narasimhaiah, A. P., Nagaraj, J. B., Pareek, P. K., Maruthikumar, N. B., & Manjunath, R. I. (2022). Implementation of NLP based automatic text summarization using spacy. International Journal of Health Sciences, 6(S5), 7508–7521. https://doi.org/10.53730/ijhs.v6nS5.10574.

[27] Seelwal, P.., Prasad. N, A.., Srinivas, C.., & V S, R. (2023). A Novel Decentralized-based Smart Contract for Merchandise Using Blockchain Technology. Journal of Online Engineering Education, 14(1), 01–12.

[28] G, M., Deshmukh, P., N. L., U. K., Macedo, V. D. J., K B, V., N, A. P., & Tiwari, A. K., (2023). Resource Allocation Energy Efficient Algorithm for H-CRAN in 5G. International Journal on Recent and Innovation Trends in Computing and Communication, 11(3s), 118–126. https://doi.org/10.17762/ijritcc.v11i3s.6172.

[29] Ramkrishna, S., Srinivas, C., Narasimhaiah, A. P., Muniraju, U., Maruthikumar, N. B., & Manjunath, R. I. (2022). A survey on blockchain security for cloud and IoT environment. International Journal of Health Sciences, 6(7), 28–43. https://doi.org/10.53730/ijhs.v6n7.10692.

International Journal of
Electrical and Electronics Research (IJEER)
Research Article | Volume 11, Issue 4 | Pages 1128-1135 | e-ISSN: 2347-470X

[30] Prakash, N. C., Narasimhaiah, A. P., Nagaraj, J. B., Pareek, P. K., Sedam, R. V., & Govindhaiah, N. (2022). A survey on NLP based automatic extractive text summarization using spacy. International Journal of Health Sciences, 6(S8), 1514–1525. https://doi.org/10.53730/ijhs.v6nS8.10526.

[31] Seelwal, P., Prasad N, A., Srinivas, C., & V S, R., (2023). Human Activity Recognition using WISDM Datasets. Journal of Online Engineering Education, 14(1s), 88–94.

[32] S. Panimalar and Dr. T. Prem Jacob (2023), Congestion-Free Cluster Formation and Energy Efficient Path Selection in Wireless Sensor Networks using ButPCNN. IJEER 11(2), 315-322. DOI: 10.37391/IJEER.110210.

[33] Praveenkumar R, Kirthika, Durai Arumugam and Dinesh (2023), Hybridization of Machine Learning Techniques for WSN Optimal Cluster Head Selection. IJEER 11(2), 426-433. DOI: 10.37391/IJEER.110224.

[34] Prathibha SB and Dr. Supriya M.C. (2023), A Novel Hybrid Energy Efficient Model using Clustering in Wireless Sensor Networks. IJEER 11(2), 451-456. DOI: 10.37391/IJEER.110227.

[35] Rekha V S and Dr. Siddaraju (2023), A Novel Buffer Packet Delivery Strategy for High Throughput and Better Health (HTBH) Method in Wireless Sensor Networks. IJEER 11(3), 866-876. DOI: 10.37391/ijeer.110334.

❖ About Authors

Dr. G N Keshava Murthy - Proposed improvised ResNet50 classification model based on re-parameterization that reduces resource consumption and model complexity by controlling the number of Residual blocks (RB) in order to achieve structured and speedy model.

Dr. Sujata Joshi - Trained the classification model with augmented dataset by using Pixel-level augmentation technique.

Dr. Rekha H – Contributed to improvise ResNet50 model which can detect and classify the brain tumor as glioma, meningioma or pituitary tumor. Proposed a hybrid segmentation model called CNN-Based Residual Block ResUnet (RB-ResUNet) with dense residual blocks to accurately locate and segment tumors region of interest (ROI) in MRI images.

Dr. Usha B S - Combined U-Net model with ResNet50 as the backbone network. At each layer, we incorporate feature and decoding module splicing. This allows the two encoding-decoding blocks to establish a stronger connection, resulting in the acquisition of more semantic information, reduction of feature redundancy, and enhancement of the model's generalization capability.

Nandini Prasad K. S - Contributed in the result analysis and experimental discussion to achieve the better model’s performance by comparing with existing work.